Coverage effects in the adsorption of H_2 on Pd(100) studied by ab initio molecular dynamics simulations

Axel Groß

Institut für Theoretische Chemie, Universität Ulm, D-89069 Ulm, Germany

The interaction of hydrogen with palladium surfaces represents one of the model systems for the study of the adsorption and *absorption* at metal surfaces. Theoretical gas-surface dynamics studies have usually concentrated on the adsorption dynamics on clean surfaces. Only recently it has become possible, based on advances in the electronic structure codes and improvements in the computer power, to address the much more complex problem of the adsorption dynamics on *precovered* surfaces. Here I present ab initio molecular dynamics (AIMD) simulations based on periodic density functional theory (DFT) calculations of the adsorption of H_2 on hydrogen-precovered Pd(100) for a broad variety of different hydrogen coverage structures. The stability of the adsorbate structures and the adsorption dynamics are analyzed in detail. Calculated sticking probabilities are larger than expected for pure site-blocking consistent with experimental results. It turns out that the adsorption dynamics on the strongly corrugated surfaces depends sensitively on the dynamic response of the substrate atoms upon the impact of the impinging H_2 molecules. In addition, for some structures the adsorption probability was evaluated as a function of the kinetic energy. Adsorbate structures corresponding to the same coverage but with different arrangements of the adsorbed atoms can lead to a qualitatively different dependence of the adsorption probability on the kinetic energy changing also the order of the preferred structures, as far as the adsorption is concerned, as a function of the kinetic energy. This indicates that dynamical effects such as steering and dynamical trapping play an important role in the adsorption on these precovered substrates.

I. INTRODUCTION

The interaction of hydrogen with palladium surfaces represents one of the model systems for the study of the adsorption at metal surfaces [1–13]. Theoretical gas-surface dynamics studies have usually concentrated on the adsorption dynamics on clean surfaces [6, 14–25]. However, in any realistic, technologically relevant situation surfaces do usually not remain clean, but are covered by adsorbates. Although the poisoning or promotion of adsorption by coadsorbates have been studied by several DFT calculations [26–31], few studies have addressed coverage effects on the adsorption dynamics [32].

Only recently it has become possible, based on advances in the electronic structure codes and improvements in the computer power, to address the complex problem of the adsorption dynamics on *precovered* surfaces either by ab initio molecular dynamics (AIMD) simulations [13, 33, 34] or by MD simulations on interpolated potential energy surfaces (PESs) [34–36]. These theoretical studies were also motivated by the experimental observation that seemingly aggregates of three or more vacancies were required for the dissociative adsorption of H_2 on almost hydrogen-covered Pd(111) [37, 38]. A subsequent DFT study indicated that the dissociative adsorption of H_2 in a hydrogen dimer vacancy should still be exothermic [39], but because of the repulsive interaction between the hydrogen atoms the dissociation is no longer non-activated but becomes hindered by small barriers. AIMD simulations then demonstrated that the dissociative adsorption of H_2 in a hydrogen dimer vacancy on Pd(111) is indeed possible once the kinetic energy is large enough to overcome the small adsorption barrier [33]. Subsequent dynamical studies of the H_2 adsorption on hydrogen-precovered Pd(100) even showed that a single hydrogen vacancy is sufficient to induce the dissociative adsorption of H_2 [34].

Preliminary results of the adsorption probability of H_2 on hydrogen-precovered Pd(100) as a function of the hydrogen coverage obtained by AIMD simulations have already been published [13, 33]. I have now extended these studies by considering a much broader variety of different hydrogen-coverage structures in the AIMD simulations. The results presented here are based on more than 6,500 AIMD trajectories for run times sometimes exceeding 100 ps demonstrating that it is indeed possible to perform a large number of AIMD simulations of surface reaction in order to obtain statistical meaningful results for a wide range of initial conditions.

The calculated sticking probabilities as a function of the coverage compare favorably with the experiment [40]. Still it should be noted that a true comparison with the experiment would require a proper statistical average over possible coverage structures and initial conditions as a function of temperature. Although I will report the relative stability of the considered hydrogen adsorbate structures as a function of the coverage, a statistical determination of the adsorption probability as a function of the coverage including the proper average over adsorbate structures is not intended in this study. This would require an even higher number of trajectories which is prohibitively expansive at the AIMD level. Such an averaging has recently been done for the H_2 adsorption on hydrogen-covered Pd(111) [35], however, not on an

AIMD basis but using an approximate reactive force-field approach to describe the interaction potential.

Here I will rather focus on the adsorption dynamics on hydrogen-precovered Pd(100) surfaces in detail in order to determine the dynamical factors determining the adsorption probability on precovered surfaces. I will contrast the adsorption probabilities for different adsorbate structures at the same coverage and thus analyze the influence of the adsorbate arrangement and thus of the lateral corrugation on the dissociative adsorption process. In addition, the dynamical response of the covered surface upon the impact of the hydrogen molecules will be discussed. For selected structures, also the dependence of the sticking probability on the initial kinetic energy has been addressed.

II. COMPUTATIONAL DETAILS

The AIMD simulations have been performed using the Vienna *Ab initio* Simulation Package (VASP) [41]. Electronic exchange and correlation has been described within the generalized gradient approximation (GGA) using the functional proposed by Perdew and Wang (PW91) [42]. Ultrasoft pseudopotentials [43, 44] have been employed to represent the ionic cores. The one-electron valence states were expanded in plane waves with an energy cutoff of 200 eV. The (100) surface was modeled by a slab of five layers with (2×2), (4×2), (3×2), and (3×3) surface unit cells in order to model different hydrogen coverages. The **k**-point sampling was performed. using Monkhorst-Pack grids of $5 \times 5 \times 1$, $3 \times 5 \times 1$ and $3 \times 3 \times 1$ **k**-points, respectively, depending on the surface unit cell.

The AIMD simulations were performed using the Verlet algorithm [45] with a time step of 1 fs within the microcanonical ensemble, i.e., the total energy was conserved during the simulations. This energy conservation was typically fulfilled to within ± 5 meV along a AIMD run. The substrate atoms were initially at rest corresponding to a surface temperature of $T_s = 0$ K, but the uppermost two layers of the Pd slab were allowed to move during the simulations.

Sticking probabilities for each considered structure and incident kinetic energy were evaluated by averaging over at least 150 trajectories which were started with random initial lateral positions and orientations of the H_2 molecule 4 Å above the surface, except for the simulations using a (3×3) surface unit cell for which only at least 100 trajectories were determined because of the larger computational effort. A trajectory was considered to correspond to a dissociation event when the interatomic distance of the molecule exceeded 2.5 Å and to a scattering event when the molecule returned to the initial distance of 4 Å from the surface. Some of the impinging molecules became trapped in molecular adsorption states in which they stayed for a rather long time, as illustrated below. Some of the trajectories have been

evaluated for run times up to 150 ps in order to determine their final fate. Still, once the energy transferred to the substrate exceeded the initial kinetic energy of the impinging molecules, they have also been considered as being adsorbed even if the eventual full dissociation was not completed.

The statistical error of the sticking probabilities amounts to $\sigma = \sqrt{S(1-S)}/\sqrt{N}$ where S is the sticking probability and N the number of trajectories [46]. For $N \geq 150$, the statistical error is $\sigma \leq 0.04$, and for $N \geq 100$, $\sigma \leq 0.05$. It is important to emphasize that the statistical error does not depend on the complexity of the system, i.e., on the number of considered dynamical degrees of freedom, but only on the number of calculated trajectories.

The H_2 molecules were initially non-vibrating, i.e, no zero-point energies were considered in the initial conditions which in fact yields a sufficient agreement between classical and quantum dynamical studies for the H_2/Pd(100) system [47]. As already mentioned, the substrate atoms were initially at rest, i.e., the initial surface temperature corresponded to 0 K. Upon adsorption, the energy transfer to the substrate leads to a heating of the substrate. The eventual temperature rise is depending on the size of the considered surface unit cell. For H_2 molecules trapped in a molecular adsorption site within a (4×2) periodicity, typically the temperature rose up by less than 10 K.

III. H_2 ADSORPTION ON CLEAN Pd(100)

Before discussing the adsorption of H_2 on H-precovered Pd(100), I will briefly review the H_2 adsorption on clean Pd(100) [13, 33]. In Fig. 1, experimentally determined sticking probabilities [2, 5] are compared to results from MD simulations. First of all, it is obvious that there is a large discrepancy between AIMD and experimental results. As already discussed [33], it might well be that surface contaminations such as hydrogen [50] or sulphur [2, 32] might have influenced the measured sticking probabilities. The discrepancy between the two sets of experimental results supports such an assumption. As we will later see, the fact that the minimum in the sticking probability measured by Rendulic *et al.* occurs at a rather high kinetic energy of about 0.3 eV might be an indication that the experiments were performed on a rather corrugated surface as for example induced by co-adsorbates. In this context I also like to note that the sticking probabilities obtained by Rendulic *et al.* in molecular beam experiments [2] for Pd(100) are well below corresponding results for Pd(111) [7, 51] which is surprising considering the fact that the more open Pd(100) is much more attractive towards H_2 dissociation compared to the densely packed Pd(111) surface [49, 52, 53].

It is also alarming that there is a quite significant difference between the MD results obtained on the PES derived from an interpolation of DFT energies and the
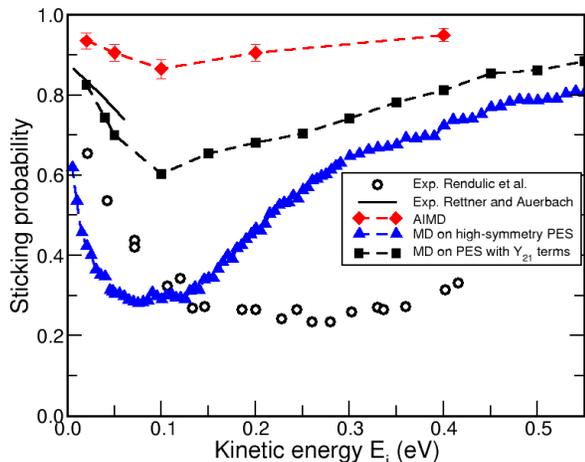
FIG. 1. Dissociative adsorption probability of hydrogen on clean Pd(100) as a function of the incident energy. The experimental results by by Rendulic *et al.* [2] and by Rettner and Auerbach [5] are compared to the results derived from *ab initio* molecular dynamics simulations. In addition, the results of MD simulations [8] performed on an interpolation of a DFT results [48, 49] obtained at high symmetry points are included. Furthermore, the results of MD simulations on this PES augmented by Y_{21} terms are plotted.

AIMD results since they are nominally based on equivalent DFT calculations (except for some technical details). However, it is important to note that the interpolation of the DFT-PES was based on high-symmetry points of the DFT, namely with the H_2 molecule above the fourfold-hollow, the bridge and the ontop position [49]. This limitation was caused by the computational constraints fifteen years ago. In fact, at all these high-symmetry configurations there is a specific symmetry $\theta \leftrightarrow \pi - \theta$ with respect to the polar orientation θ of the molecular axis. This is closely related to the fact that at these sites it is energetically most favorable to have the H_2 molecular axis parallel to the surface. However, for an arbitrary position within the surface unit cell, this symmetry is in general not fulfilled.

In order to estimate the error induced by this additional artificial symmetry $\theta \leftrightarrow \pi - \theta$ I added a term

$$V_{21}(Z, X, Y, \theta, \phi) = V_{21}(Z)(\sin GX \cos \phi - \sin GY \sin \phi) \sin 2\theta \tag{1}$$

to the original parameterization of the H_2/Pd(100) PES [8], where X, Y, Z are the three cartesian coordinates of the H_2 center of mass position and θ and ϕ are the polar and azimuthal orientation of the molecular axis, respectively, and $G = 2\pi/a$ is the length of the basis vectors of the two-dimensional reciprocal space of the (100) surface. Note that because of

$$Y_{21}(\theta, \phi) + Y_{2-1}(\theta, \phi) \propto \sin 2\theta \cos \phi ,$$
$$Y_{21}(\theta, \phi) - Y_{2-1}(\theta, \phi) \propto \sin 2\theta \sin \phi \tag{2}$$

the potential term in Eq. 1 was denoted V_{21}. Instead of reparameterizing the whole PES I just added this term

with an maximum variation of ± 1 eV to the original PES. This value was estimated based on DFT calculations.

The potential $V_{21}(Z, X, Y, \theta, \phi)$ has a mean value of 0 eV, i.e., its addition hardly modifies the distribution of the barrier heights towards dissociative adsorption. Still, its consideration strongly enhances the resulting sticking probability, as the results of the MD simulation including the Y_{21} term plotted in Fig. 1 demonstrate. In fact, the agreement with the AIMD data is much better. This indicates that the strong discrepancy between AIMD and original MD data is due to the additional artificial symmetry included in the original parameterization used for the MD simulations. Adding the Y_{21} term makes the anisotropy and the corrugation of the PES larger; therefore the effects of steering and dynamical trapping [20, 21] becomes much stronger which leads to the higher sticking probability.

It should be noted that the dissociation dynamics on a PES with a coexistence of non-activated and activated paths towards adsorption depends sensitively on the details of the multidimensional PES [54, 55] since a broad region of the configuration space is probed by the impinging molecules. For an activated system, apparently only the region close to the minimum barrier matters. This is indicated by the fact that for the adsorption of H_2 on (2×2) sulphur-covered Pd(100) the results of AIMD simulations [13] and MD simulations [32, 56] on a parameterized PES derived from DFT calculations [27], also including the artificial symmetry $\theta \leftrightarrow \pi - \theta$, hardly differ.

IV. ENERGETICS OF THE H_2 ADSORPTION ON H-PRECOVERED Pd(100)

In order to illustrate the effect of the hydrogen coverage on the dissociation of additional impinging H_2 molecules I have collected some two-dimensional cuts through the potential energy surface (PES) for the H_2 dissociation in Fig. 2. Shown are so-called elbow plots as a function of the H_2 center of mass distance Z from the surface and the H-H spacing d. In Fig. 2a, the dissociation path in a bridge-hollow-bridge (bhb) configuration on clean Pd(100) is depicted, i.e., the H_2 center of mass is above a hollow position, and the H atoms are propagating towards the bridge sites. This path is slightly activated at the clean surface [48, 49].

If an adsorption site is occupied with an hydrogen atom, then this site is blocked for further adsorption. Two hydrogen atoms ontop of each other at the fourfold hollow site are in fact 880 meV more costly than at their maximum distance within the (4×4) surface unit cell [57]. However, also the H_2 dissociation barrier is significantly enhanced above an adsorbed hydrogen atom, as Fig. 2b illustrates for the H_2 dissociation within a bhb geometry for which a barrier of 1.7 eV results.

Adsorbed hydrogen atoms also influence the energetics of the adsorption of further hydrogen molecules in neighboring sites, as Fig. 2c demonstrates. The barrier for the
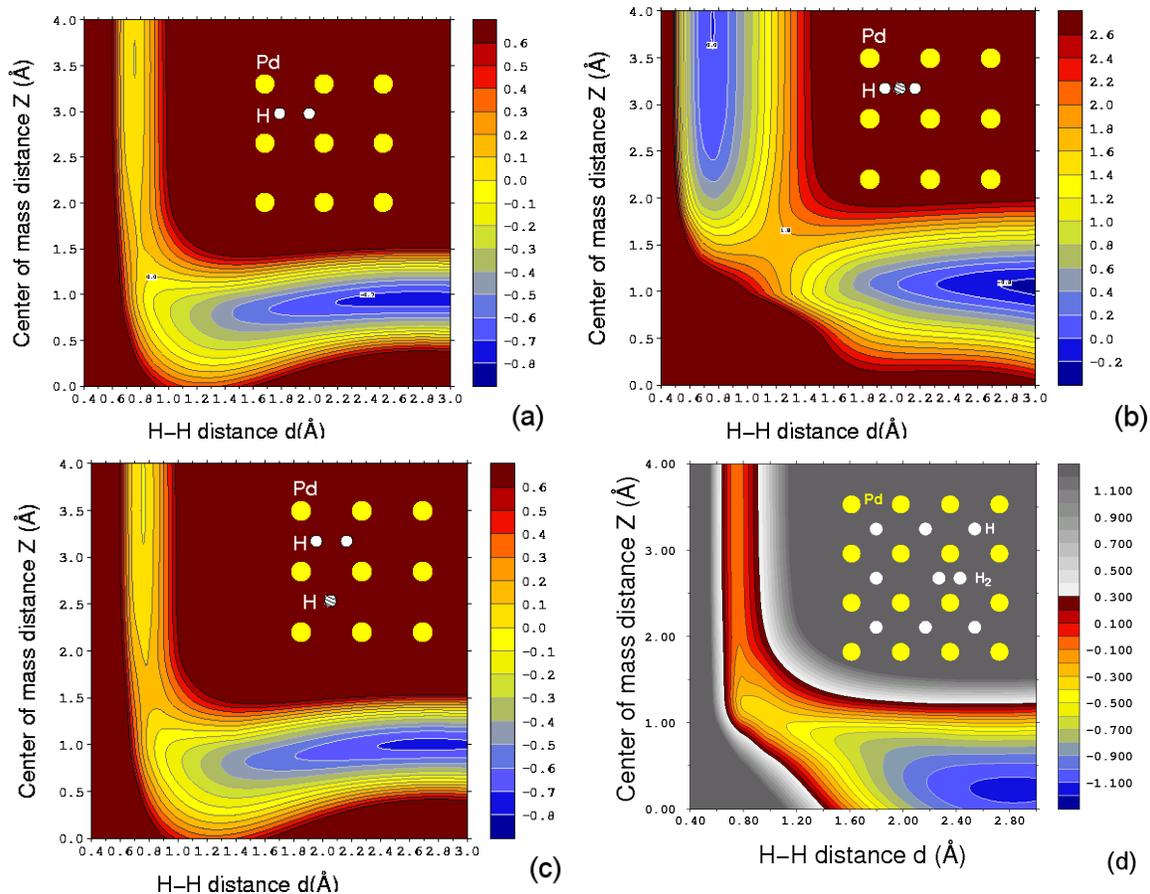
FIG. 2. Two-dimensional cuts through the potential energy surface for H_2 dissociation on clean and hydrogen covered Pd(100) as a function of the H_2 center of mass distance from the surface and the H-H spacing. a) H_2 dissociation at clean Pd(100) in a (2×2) geometry in a bridge-hollow-bridge (bhb) configuration; b) H_2 dissociation above an adsorbed hydrogen atom on Pd(100) in a (2×2) geometry in a bhb configuration; c) H_2 dissociation adjacent to an adsorbed hydrogen atom on Pd(100) in a (2×2) geometry in a bhb configuration; d) H_2 dissociation in a hydrogen divacancy of a hydrogen-precovered $7H(3 \times 3)$/Pd(100) surface in a hollow-bridge-hollow configuration. The energy spacing of the contour lines is indicated besides the figures, in a), c) and d) it is $0.1\,\mathrm{eV}$, in b) it is $0.2\,\mathrm{eV}$. The adsorption geometries are indicated in the insets in each panel.

bhb dissociation path is increased by $0.1\,\mathrm{eV}$ compared to clean surface if the adjacent hollow site is occupied by a hydrogen atom. Yet, in spite of this repulsive interaction the H_2 dissociation into a hydrogen divacancy on an almost H-covered Pd(100) surface is still non-activated, in contrast to Pd(111) [39]. Figure 2d shows the elbow plot of H_2 dissociation in a hydrogen divacancy of a hydrogen-precovered $7H(3 \times 3)$/Pd(100) surface in the hollow-bridge-hollow (hbh) configuration. Although the minimum energy path towards dissociative adsorption is less attractive than the corresponding hbh path on clean Pd(100) [48, 49], there is no barrier along this path. Finally it should also be noted that on hydrogen-precovered Pd(100) the non-activated adsorption of an impinging H_2 molecule in a single hydrogen vacancy is possible with one hydrogen atom ending in the four-fold hollow site and the other one in an adjacent bridge site [34].

V. H_2 ADSORPTION DYNAMICS ON HYDROGEN-PRECOVERED Pd(100)

A. Overview

In total, I have determined the sticking probability of H_2 impinging on hydrogen-covered Pd(100) for coverages $\Theta_H = 1/4, 1/3, 1/2, 5/9, 2/3, 3/4$ and $7/9$, respectively. The corresponding calculated relative sticking probabilities $S(\Theta)/S(0)$ determined for an incident kinetic energy of $E_{\mathrm{kin}} = 0.1\,\mathrm{eV}$ are summarized in Fig. 3 and compared to experimental results for an H_2 gas [40]. This particular kinetic energy has been chosen as a compromise, being somewhat larger than typical thermal energies but not too large so that still steering and dynamical trapping can occur. The various calculated results at the same coverage are obtained for different adsorbate structures; they are discussed in detail in the following. The different considered coverage structures are numbered consec-
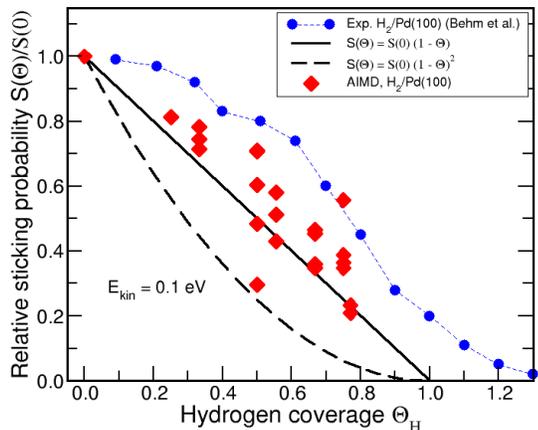
FIG. 3. Relative dissociative adsorption probability $S(\Theta)/S(0)$ of hydrogen on hydrogen-covered Pd(100) as a function of the coverage. The theoretical results are obtained for an initial kinetic energy of $0.1\,\mathrm{eV}$ at different configuration of the adsorbed hydrogen atoms whereas the experimental results by by Behm *et al.* [40] are measured using an ????
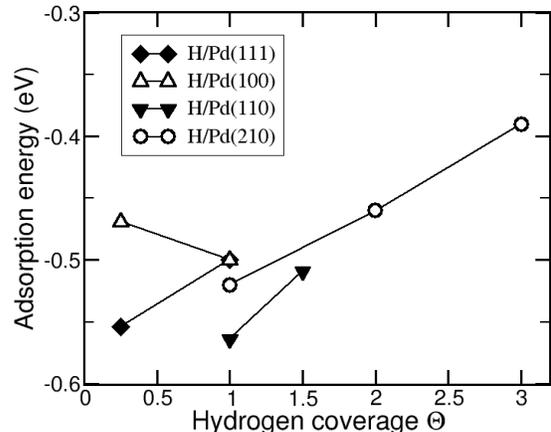

FIG. 4. H adsorption energies in eV per atom with respect to the free H_2 molecule based on various DFT calculations for the most favorable adsorption sites on Pd(100) and Pd(111) [58], on Pd(110) [59], and on Pd(210) [30].

utively and illustrated in Figs. 5-13. The experimental results are larger than the calculated ones. It has to be noted that the experiments were performed using an H_2 gas whereas the simulations correspond to a molecular beam setup with a mono-energetic beam. Furthermore, no internal excitations such as vibrations or rotations have been considered in the initial conditions of the AIMD simulations. Still it is satisfying that the calculated results are enveloped by the measured sticking probabilities indicating that the qualitative trends as a function of the coverage are reproduced.

Furthermore, all calculated results were obtained for a particular periodic arrangement of adsorbed hydrogen atoms within relatively small surface unit cells. For a realistic description of the experiment, a proper thermal distribution of the adsorbed hydrogen structures should be taken into account, as recently done for the H_2 adsorption on H-covered Pd(111) using a reactive force field for the description of the interaction potential [35]. In the following, I will report the relative stability of the considered adsorbate structures. Still, as mentioned in the introduction, I have made no attempt to perform any statistical average since the number of considered structures is still too small. In the following, I will rather focus on the general trends in the adsorption dynamics on precovered surfaces.

In addition, two curves corresponding to $S(\Theta_H) = S(0)(1-\Theta_H)$ and $S(\Theta_H) = S(0)(1-\Theta_H)^2$ are included in Fig. 3 which would correspond to the sticking probability if it was determined by pure site-blocking requiring one or two empty sites, respectively. All measured sticking probabilities and most of the calculated sticking probabilities of H_2 on Pd(100) are larger than the values predicted from a simple site-blocking picture. This suggests

that the repulsive interaction between the impinging hydrogen molecules and the adsorbed hydrogen atoms, as indicated in Fig. 2, is overcompensated by dynamical effects.

Note that for the H_2 adsorption on hydrogen-precovered Pd(111), a qualitatively different dependence of the sticking probability is observed [35, 60, 61], the sticking probability lies at or below the $(1 - \Theta_H)^2$ curve. This can be explained by the differences in the adsorption energies as a function of the coverage. In Fig. 4, I have collected adsorption energies of hydrogen as a function of the coverage based on various DFT calculations for the most favorable adsorption sites on Pd(100) and Pd(111) [58], on Pd(110) [59], and on Pd(210) [30]. There is a general trend obvious that the binding becomes weaker for higher coverages due to the mutual repulsion. The hydrogen adsorption energies on Pd(100) represent an exception. At the four-fold hollow site, the hydrogen adsorption are practically independent of the coverage. This is caused by the fact that the hydrogen atoms at the rather open four-fold hollow sites are adsorbed at almost the same height as the surrounding Pd atoms [48, 49] leading to an effective screening of the hydrogen atoms and a hydrogen adsorption energies that is rather weakly dependent on the coverage.

B. $\Theta_H = 1/4$

The hydrogen coverage of $\Theta_H = 0.25$ has been realized within a (2×2) surface unit cell. The resulting relative sticking probability $S(\Theta_H = 0.25)/S(0) = 0.81$ is larger than the $S(0)(1-\Theta_H)$ and $S(0)(1-\Theta_H)^2$ values. This enhancement is caused by the fact that at this open structure, H_2 molecules impinging close to the occupied adsorption site can be effectively steered to empty ad-
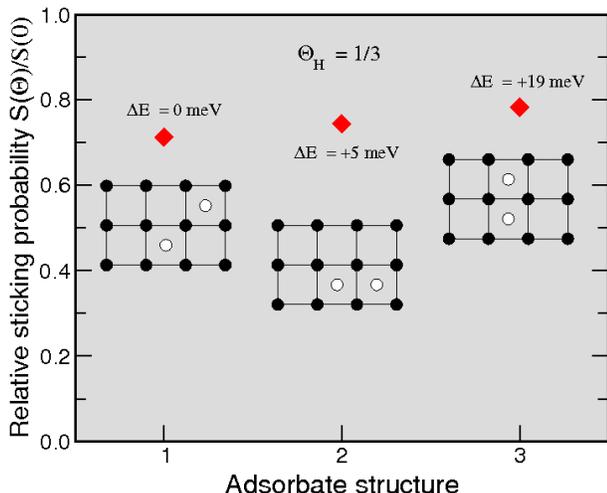
FIG. 5. Calculated relative dissociative adsorption probability $S(\Theta)/S(0)$ of hydrogen on hydrogen-covered Pd(100) with a coverage of $\Theta_H = 0.33$ for three different adsorbate structure within a (3×2) periodicity as indicated in the insets. In addition, the stability ΔE in meV of the adsorbate structures per hydrogen atom with respect to the most favorable structure is given in the figure.
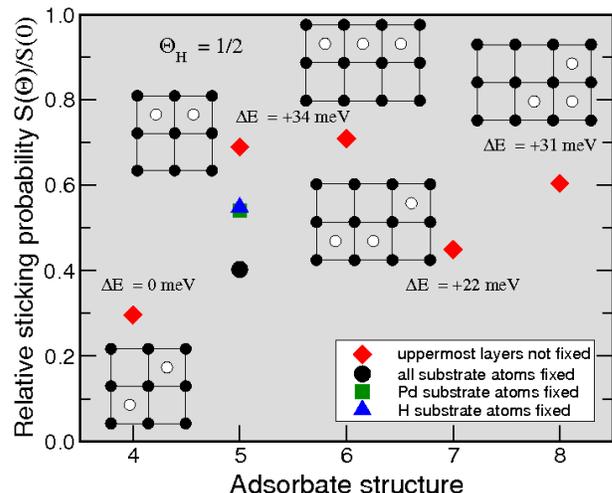

FIG. 6. Calculated relative dissociative adsorption probability $S(\Theta)/S(0)$ of hydrogen on hydrogen-covered Pd(100) with a coverage of $\Theta_H = 0.5$ for two different adsorbate structure within a (2×2) periodicity for three different adsorbate structure within a (3×2) periodicity as indicated in the insets. Furthermore, for structure **5** the results of AIMD simulations with the adsorbed hydrogen atoms, the Pd atoms or all substrate atoms kept fixed, respectively. In addition, the stability ΔE in meV of the adsorbate structures per hydrogen atom with respect to the most favorable structure is given in the figure.

sorption sites, as an analysis of the trajectories reveals.

C. $\Theta_H = 1/3$

I have considered three different H adsorbate structures with a coverage $\Theta_H = 1/3$ within a (3×2) geometry which are depicted in Fig. 5 together with their relative stability with respect to the most favorable structure **1**. The most favorable structure is the one where the two hydrogen atoms are second-nearest neighbors thus minimizing their mutual repulsion, whereas the most unfavorable structure **3** consists of a striped phase with a hydrogen row along a nearest-neighbor direction. On the other hand, this striped phase shows the highest sticking probability obviously because of its open structure with two adjacent rows of vacant adsorption sites. Still, the differences in the sticking probabilities are relatively small but statistically significant.

D. $\Theta_H = 1/2$

In Fig. 6, the relative sticking probabilities are plotted for five different structures with a coverage $\Theta_H = 1/2$ within a (2×2) geometry and a (3×2) geometry, respectively. As far as the stability is concerned, again the structures with the lowest number of nearest neighbor adsorbates are energetically preferred. Among the considered structure with $\Theta_H = 1/2$ this is structure **4** in which no hydrogen atoms are adsorbed in nearest-neighbor sites.

In fact, in this structure **4**, there are also no adjacent vacant adsorption sites. Still, dissociative adsorption of impinging H_2 molecules can occur. Almost all of the impinging H_2 molecules that eventually dissociate become first trapped in a molecular adsorption well ontop of a Pd atom, as already discussed in Refs. [13, 33, 34]. The dissociation then proceeds with one hydrogen atom entering the fourfold-adsorption site with the other hydrogen atom first remaining at an adjacent bridge.

Such a process is illustrated in Fig. 7 by snapshots along a trajectory impinging on a H-covered surface corresponding to structure **7** which also exhibits this adsorbate pattern with occupied second-nearest neighbor sites. For more than 30 ps, the H_2 molecule becomes trapped in the molecular adsorption well above a Pd atom (Fig. 7a) after impinging on the surface with an initial kinetic energy of $E_{kin} = 0.1$ eV. After about 35 ps, one of the hydrogen atoms enters the fourfold hollow site while the other atom stays at the bridge site (Fig. 7b). At such a bridge site, between two occupied fourfold hollow sites, the hydrogen atom stays in a metastable state. In can propagate away from this site, but only in an exchange-like fashion. The adsorption into an isolated vacancy has already been addressed in a study combining MD simulations on an interpolated PES derived from DFT calculations and AIMD simulations [34]. This showed that not two or even three adjacent vacancies, as recently suggested [37], are required for the dissociative adsorption of H_2 on Pd surfaces, one isolated vacancies is in fact
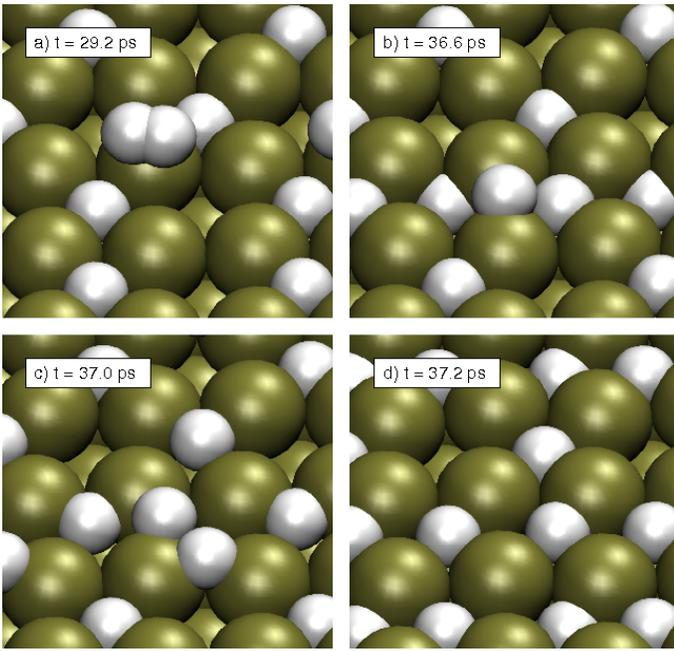
FIG. 7. Snapshots of an AIMD trajectory of H_2 impinging on hydrogen-precovered Pd(100) with an initial kinetic energy of 100 meV. The initial hydrogen coverage is $\theta_H = 1/2$ within a (3×2) surface periodicity corresponding to structure **7**.

FIG. 8. Comparison of two trajectories with identical initial conditions on a H-precovered ($\Theta_H = 0.5$) Pd(100) surface with all substrate atoms fixed and with only the preadsorbed H substrate atoms kept fixed, respectively. Plotted are the H_2 center of mass distance from the surface in Å, the total kinetic energy of the impinging H_2 molecule and the kinetic energy of the Pd atoms.

sufficient to induce the dissociative adsorption of H_2.

It should be noted that the kinetic energy gain that occurs when one hydrogen atom enters the fourfold hollow site is quickly distributed among the other hydrogen atoms on the surface, however, due to the large mass mismatch between H and Pd atoms the energy equilibration with the metal atoms is much slower [62]. Upon a suitable fluctuation of the adjacent hydrogen atom in the adsorption site, the hydrogen atom from the bridge site can enter this site while the H atom originally occupying the site hops to the next vacant site (Fig. 7c) so that the dissociative adsorption event is eventually completed (Fig. 7d). In fact, I have run basically all trajectories until the final fate of the interaction event was decided which took up to 150 ps. The existence of the atomic hydrogen adsorption state at the bridge sites of an almost fully hydrogen-covered Pd(100) surface might be experimentally detectable.

As far as the sticking probability of all considered structures in Fig. 6 is concerned, we see again an anticorrelation with the energetical stability of the coverage structures: The striped structure that is the least stable exhibits the higher sticking probability. Note that structures **5** and **6** are in principle equivalent, only the surface unit cell is different. It is comforting that within the statistical uncertainty $\leq \pm 0.04$ the sticking probabilities are the same. Structure **8** has a slightly smaller sticking probability than the striped structure but all vacancies have another vacancy as a nearest-neighbor. In contrast,
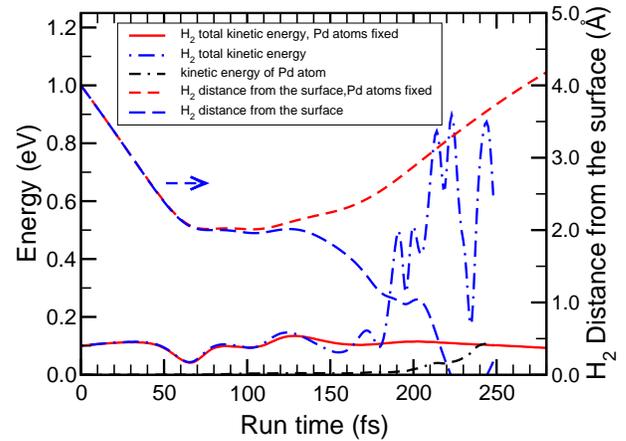
in structure **7** there is an isolated vacancy apart from a divacancy which leads to the reduced sticking probability.

In order to better understand the role of the substrate degrees of freedom in the adsorption process, for the (2×2) structure **5** we have additionally performed AIMD simulations with the adsorbed hydrogen atoms, the Pd atoms or all substrate atoms kept fixed, respectively. As Fig. 6 shows, the sticking probability is almost reduced by a factor 1/2 when all substrate atoms are kept fixed. This seems to be understandable by the fact that due to the presence of the precovered hydrogen atoms the impinging H_2 molecules can efficiently transfer their energy to the substrate because of the similar masses. This transferred energy is then not available for the scattering thus increasing the adsorption probability. Note that on clean Pd(100), such an energy transfer only plays a minor role because of the large mass mismatch between impinging H_2 molecules and the Pd substrate atoms [33].

However, a smaller but similar reduction of the sticking probability results if only the hydrogen adsorbate atoms or only the Pd atoms are kept fixed. This is surprising because it means that for these two different scenarios the arguments invoking an appropriate mass ratio do obviously not hold. I have analyzed some trajectories more closely in order to identify the role of the Pd substrate atoms in the dissociative adsorption. In Fig. 8, two trajectories with the same initial conditions are depicted, in the one case with all Pd and H substrate atoms kept fixed, in the other case with only the H substrate atoms kept fixed, i.e., with the Pd substrate atoms allowed to move. For the whole substrate being fixed, the impinging H_2 molecule is scattered back into the gas phase whereas the molecule adsorbs dissociatively when the Pd atoms are allowed to move. Analyzing the plotted distance of

the H_2 molecule from the surface, it becomes obvious that after 100 fs the two trajectories start to differ, and at about 120 fs the molecule impinging on the fixed substrate starts to return to the gas phase whereas the other molecule begins to approach closer to the surface and finally adsorb dissociatively which is reflected by the large and oscillatory increase in the H_2 kinetic energy. However, it is also obvious that the energy transfer to the Pd atoms only starts when the H atoms enter the adsorption site and become strongly accelerated. This means that at the time when the fate of the trajectory, scattering or adsorption, is decided, there is no significant energy transfer to the substrate Pd atoms.

Thus the energy transfer argument is not applicable in the analysis of the two trajectories. Instead, rather other dynamical arguments have to be invoked that do not involve energy transfer. Note that due to the presence of the preadsorbed hydrogen atoms the potential energy surface of the H_2 molecules is much more corrugated than the PES for H_2 interacting with clean Pd(100), similar to the situation of H_2 impinging on sulfur-precovered Pd(100), as already discussed [27, 32]. This strong corrugation leads to strong steering effects which are very sensitive to the particular arrangement of the substrate atoms. Note also that any single trajectory sensitively depends on the initial conditions, i.e., the interaction dynamics is highly non-linear and chaotic. Hence, it is a small rearrangement of the Pd substrate atoms upon the impact of the H_2 molecules that does not show up in the energy balance which changes the fate of the trajectory. This argument not invoking any energy transfer is consistent with the observation that there are also few trajectories with the same initial conditions that lead to dissociative adsorption on the fixed substrate but to scattering when the Pd substrate atoms are allowed to move.

The H_2 adsorption for structures **4** and **5** was in fact also considered in molecular dynamics simulations using an interpolated PES [34] obtained within the corrugation reducing procedure (CRC) [63]. Similar, but slightly smaller values for the relative sticking probabilities of about 0.25 for structure **4** and of about 0.55 for structure **5** were obtained in these CRC-MD simulations [34]. However, these simulations were performed including the zero-point energy (ZPE) in the H-H vibrations in the initial conditions on a fixed substrate which corresponds to so-called quasi-classical trajectories. While the inclusion of the vibrational ZPE leads to an increase in the sticking probability due to vibrational softening [34, 47, 64], the neglect of surface recoil reduces the sticking probability of H_2 on H-precovered Pd(100), as just discussed. Hence these two sets of results are consistent.

In order to get further insight into the adsorption dynamics on the precovered surface, I have determined the sticking probability as a function of the kinetic energy at the hydrogen-coverage structures **6**, **7**, and **8** based on AIMD simulations. The sticking probabilities are plotted in Fig. 9 and compared to the results on clean Pd(100).

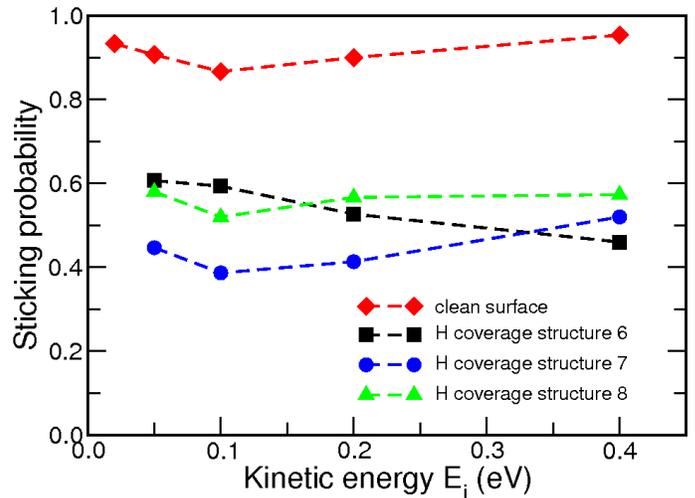First of all it is obvious that the sticking probabili-

FIG. 9. Dissociative adsorption probability of hydrogen on clean and hydrogen-covered Pd(100) derived from AIMD simulations as a function of the incident energy. The hydrogen-covered structures with $\Theta_H = 1/2$ within a (3×2) geometry are illustrated in the insets of Fig. 6.

ties at the various adsorbate structures exhibit a qualitatively different dependence of the incident kinetic energy. At structure **6**, the sticking probability monotonically decreases, and at structures **7** and structure **8** it exhibits a non-monotonic behavior with the minimum at $E_{kin} = 0.1\,eV$ as a function of the kinetic energy. A decrease of the sticking probability as a function of kinetic energy in the dissociative adsorption probability of H_2 on metal surfaces is typically an indication that steering effects and dynamical precursors are present [8, 14, 20–22] which become suppressed at higher kinetic energies. Interestingly enough, at the stripe-like structure the decrease continues up to kinetic energies of 0.4 eV where the sticking probability even drops below the value for pure site blocking $S(\Theta_H) = S(0)(1 - \Theta_H)$. It also becomes smaller than the sticking probability at the other two considered structures with $\Theta_H = 1/2$.

At clean metal surfaces with non-activated hydrogen adsorption, the minimum of calculated sticking probabilities typically occurs at lower kinetic energies of about 0.1 to 0.2 eV [14, 20, 65–68]. However, we have to take into account that at precovered surfaces the corrugation is much larger than at clean surfaces. In particular in structure **6**, there are rows of occupied and of vacant adsorption sites alternating, creating a rather pronounced difference. In addition, molecules steered towards the vacancy rows will always find vacant adsorption sites with two vacant nearest-neighbor sites. This is different in particular for structure **7**, but also for structure **8**, where steering can occur to less favorable adsorption sites so that the scattering probability becomes larger. Structure **7** corresponds to a single plus a dimer vacancy, there is no vacancy row. Hence the poisoning of the access towards the adsorption sites is most pronounced for this
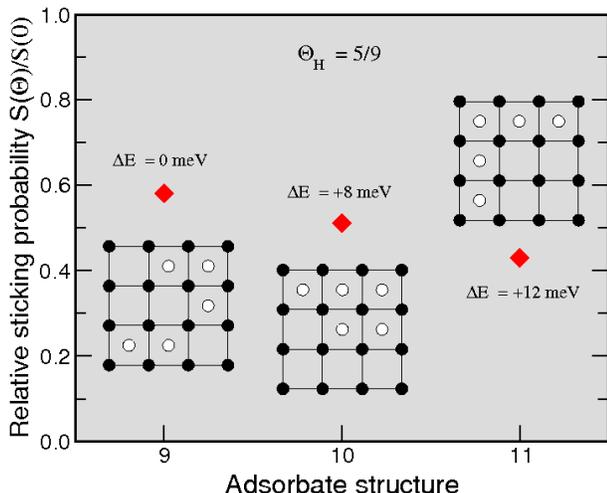
FIG. 10. Calculated relative dissociative adsorption probability $S(\Theta)/S(0)$ of hydrogen on hydrogen-covered Pd(100) with a coverage of $\Theta_H = 5/9$ for three different adsorbate structure within a (3×3) periodicity as indicated in the insets. In addition, the stability ΔE in meV of the adsorbate structures per hydrogen atom with respect to the most favorable structure is given in the figure.

structure which leads to the small sticking probability of this structure. However, at higher kinetic energies the dynamical effects play a less important role so that the sticking probabilities of all considered structures become rather similar.

I like to draw the attention to the fact that the minimum in the sticking probability measured by Rendulic *et al.* [2] was found at a kinetic energy of about $0.3\,\text{eV}$, at a higher energy than for structures **6** and **7**. This might be an indication that the substrate in the experiment was poisoned by coadsorbates such as sulphur leading to a strongly corrugated surface which extends the regime of kinetic energies in which steering and dynamical trapping effects are operative to higher energies.

The dependence of the sticking probability on the initial kinetic energy on H-covered Pd(100) with $\Theta_H = 1/2$ was also determined in the CRC-MD simulations, but just for structures **4** and **5** [34]. For the $c(2 \times 2)$ structure **5**, an activated behavior analogous to the curve determined here for structure **7** was found. However, for structure **5**, a dependence of the sticking probability similar to the curve here obtained for structure **8** was found whereas it should be in principle similar to the one obtained here for structure **6**. Please recall that in these simulations quasiclassical trajectories on a fixed substrate were run so that the results are not directly comparable to the AIMD runs, as far as dynamical aspects are concerned.

E. $\quad \Theta_H = 5/9$

Three different H adsorbate structures with an coverage $\Theta_H = 5/9$ within a (3×3) geometry have been considered. They are illustrated in Fig. 10. With respect to their relative stability, structure **9** is energetically most favorable, again because it is the structure with the least number of hydrogen atoms at nearest-neighbor sites. However, here we have the unusual situation that the most stable adsorbate structure also exhibits the highest adsorption probability whereas so far we usually had an anti-correlation between stability and sticking probability. It is also rather surprising that structure **11** has the lowest sticking probability although there are four connected vacancies. However, Fig. 9 already demonstrated that because of dynamical effects the order in the sticking probability among different structures can be altered.

Note that structure **11** has a compact square structure of four adjacent vacancy, however, there are also compact connected square structures of five adjacent occupied sites with one hydrogen atom at the center which are rotated by $45°$ with respect to the (3×3) cell depicted in Fig. 10. An analysis of the trajectories of H_2 molecules impinging on structure **11** reveals that the majority of them are repelled from this hydrogen structure but not steered towards the vacancy island. Structure **9**, on the other hand, has a small L-shaped vacancy island consisting of three sites where molecules can directly dissociate. In addition, H_2 molecule impinging on the hydrogen-covered regions can also be redirected towards the additional hydrogen vacancy which is surrounded by occupied sites, and there the H_2 molecules can dissociate in a two-step mechanism as illustrated in Fig. 7.

F. $\quad \Theta_H = 2/3$

The H adsorbate structures corresponding to a coverage $\Theta_H = 2/3$ were also realized using a (3×3) geometry, i.e. there were six adsorbed hydrogen atoms per surface unit cell. The considered structures are illustrated in Fig. 11. We find the well-known pattern, as far as the energetical stability is concerned: The structure **12** with the least number of occupied nearest-neighbor adsorption sites is most stable. There is symmetry in this stability argument with respect to occupied and unoccupied sites because the number of occupied nearest-neighbor sites is directly related to the number of nearest-neighbor vacancy sites. Thus one could also say that there is a repulsive interaction between the vacancies and that the structure with the least number of nearest-neighbor vacancy sites is the most stable one. This is clearly structure **12** where no dimer vacancy is present.

Consequently, there is no direct dissociative adsorption into a dimer vacancy possible in structure **12**, and hence, the dissociation probability is smaller than for the structures with adjacent vacancies. Still, structure **13** exhibits the same sticking probability within our statistical
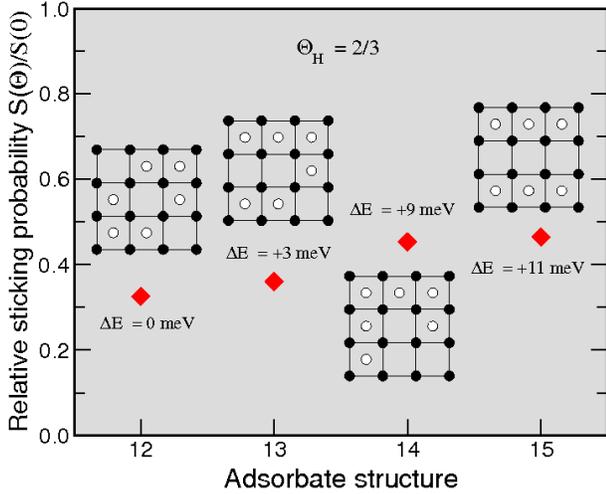
FIG. 11. Calculated relative dissociative adsorption probability $S(\Theta)/S(0)$ of hydrogen on hydrogen-covered Pd(100) with a coverage of $\Theta_H = 2/3$ for three different adsorbate structure within a (3×3) periodicity as indicated in the insets. In addition, the stability ΔE in meV of the adsorbate structures per hydrogen atom with respect to the most favorable structure is given in the figure.
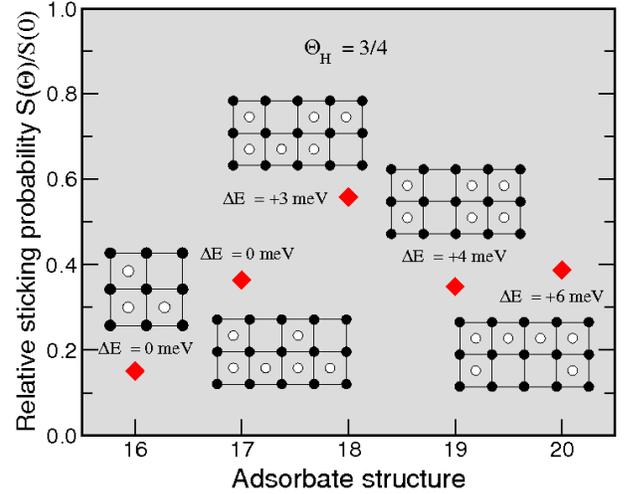

FIG. 12. Calculated relative dissociative adsorption probability $S(\Theta)/S(0)$ of hydrogen on hydrogen-covered Pd(100) with a coverage of $\Theta_H = 3/4$ for five different adsorbate structure within a (2×2) and (4×2) periodicity, respectively, as indicated in the insets. In addition, the stability ΔE in meV of the adsorbate structures per hydrogen atom with respect to the most favorable structure is given in the figure.

uncertainty, since there is only one dimer vacancy.

G. $\Theta_H = 3/4$

The H adsorbate structures corresponding to a coverage $\Theta_H = 3/4$ were realized using both a (2×2) and a (4×2), as shown in Fig. 12. The most stable structure **16** which is also considered as the (4×2) structure **17** consists of isolated hydrogen vacancies whereas structure **19** with a line of vacancies and structure **20** with an isolated divacancy are higher in energy, indicative of a repulsion between the vacancies. Structure **18** also consists of two isolated vacancies that are even further away from each other than the vacancies in structure **17**. Still, surprisingly structure **18** is energetically less favorable than structure **17**. The reasons for this energetic difference remain unclear and require further investigation.

The sticking probabilities for the (2×2) and (4×2) geometry structures **16** and **17** should in principle be the same since they correspond to the same coverage pattern. Still they differ by a factor of two. It is true that in structure **16** no dissociative adsorption into two vacancies is possible since there is only one vacancy per impinging H_2 molecule present in the (2×2) structure. On the other hand, whenever one of the hydrogen atoms of the impinging H_2 molecule enters a fourfold hollow site, the molecule does eventually fully dissociate and not scatter back into the gas phase, as the AIMD simulations on structure **17** show. Hence it can only be the mutual repulsion between the H_2 molecules within the (2×2) periodicity that leads to the reduced sticking probability of structure **16** compared to structure **17**.

Recall that for structures **5** and **6** which correspond to the same coverage arrangement within a (2×2) and a (3×2) periodicity, respectively, we found the same sticking probability indicating that for these structures the H_2 interaction with its periodic images is negligible. However, one has to note that the latter structures with a coverage of $\Theta_H = 1/2$ are more open so that the impinging H_2 molecules more quickly enter the chemisorption sites whereas on the denser structures **16** and **17** the impinging molecules are rather often trapped in dynamical molecular precursor states above ontop sites. Apparently at these sites there is a much stronger repulsion than between hydrogen atoms adsorbed in the fourfold hollow sites of Pd(100) within the (2×2) geometry which leads to a reduction of the sticking probability.

The H_2 adsorption on structure **16** was also considered in CRC-MD simulations [34] discussed already in the section covering $\Theta_H = 1/2$. Again these results obtained using quasi-classical trajectories on a fix substrate are similar to the AIMD results, since the promoting effect of the inclusion of vibrational zero-point energy [34, 47, 64] apparently cancels the opposing effect of neglecting surface recoil.

It is also surprising that the sticking probability for structure **18** is significantly larger than the sticking probability for the other structures with a (4×2) periodicity which are rather similar. The vacancies in structure **18** have the largest mutual distance of all considered structures. In other words, these vacancies are most uniformly distributed. For example, structure **18** is the only structure in which every hydrogen atom has a vacancy as a nearest-neighbor site. This leads to the steering of many impinging H_2 molecules towards a vacancy site as an in-
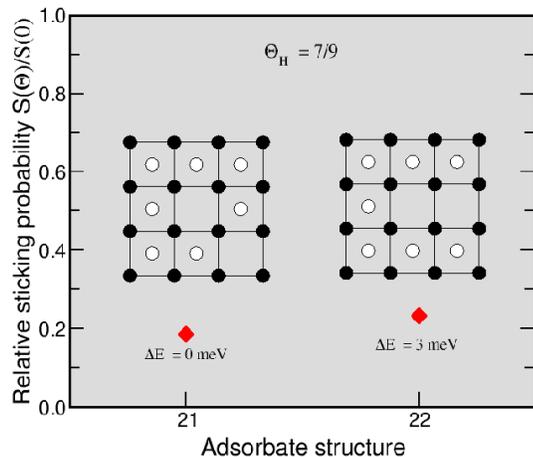
FIG. 13. Calculated relative dissociative adsorption probability $S(\Theta)/S(0)$ of hydrogen on hydrogen-covered Pd(100) with a coverage of $\Theta_{\mathrm{H}} = 7/9$ for two different adsorbate structure within a (3×3) periodicity as indicated in the insets. In addition, the stability ΔE in meV of the adsorbate structures per hydrogen atom with respect to the most favorable structure is given in the figure.

spection of the trajectories reveals.

H. $\quad \Theta_{\mathrm{H}} = 7/9$

Finally we consider a hydrogen coverage of $\Theta_{\mathrm{H}} = 7/9 \approx 0.778$ which has been achieved within a (3×3) geometry by distributing seven hydrogen atoms over the nine adsorption sites. In other words, two vacancies are distributed within a (3×3) supercell. In fact, only two inequivalent situations can be created for such a setup with the vacancies either at next-nearest neighbor sites (structure **21**) or at nearest-neighbor sites (structure **22**) (see Fig. 13). Again, the structure without nearest-neighbor vacancies is energetically more favorable. Note that the energy difference per hydrogen atom between structures **21** and **22** is the same as between structures **12** and **13** for $\Theta_{\mathrm{H}} = 2/3$ (see Fig. 11) which makes sense since the structural differences are also very similar. The sticking probability for structure **21** is slightly smaller than the one for structure **22**, but within the statistical uncertainty both sticking probabilities should be considered to be equal. This is also consistent with the results for $\Theta_{\mathrm{H}} = 2/3$, as far as structures **12** and **13** are con-

cerned.

VI. CONCLUSIONS

The adsorption dynamics of H_2 on hydrogen-precovered Pd(100) has been studied for a broad variety of different coverage structures using ab initio molecular dynamics simulations based on density functional theory calculations. Furthermore, the energetic stability of the coverage structures has been determined. Structures with either hydrogen adatoms or vacancies, respectively, as nearest neighbors turned out to be energetically slightly less favorable than other structures with more evenly distributed hydrogen adatoms or vacancies, respectively, indicative of a weak repulsion. Typically, the hydrogen coverage structures with a large number of adjacent vacancies exhibit a larger sticking probabilities than those with isolated vacancies. The dynamical response of the substrate atoms upon the impact of the impinging H_2 molecules plays an important role in the adsorption dynamics. Still, a more even distribution of isolated vacancies also promotes dissociation through steering effects towards the vacancies. The higher sticking probability at such structures is amplified by the fact that on hydrogen-covered Pd(100) a single vacancy can induce the dissociative adsorption of H_2. The H atom not entering the vacancy first occupies an adjacent bridge site and then diffuses in an exchange-mechanism to an empty fourfold adsorption site. However, the order of the more favorable coverage structures with respect to the sticking probability can change as a function of the kinetic energies indicating the importance of dynamical effects in the H_2 adsorption. Altogether, dynamical recoil and steering effects lead to a H_2 sticking probability on H-precovered Pd(100) that is much larger than expected from a pure site-blocking picture, in agreement with experiment.

[1] K. Christmann, Surf. Sci. Rep. **9**, 1 (1988).
[2] K. D. Rendulic, G. Anger, and A. Winkler, Surf. Sci. **208**, 404 (1989).
[3] K. D. Rendulic and A. Winkler, Surf. Sci. **299/300**, 261 (1994).
[4] M. Beutl, M. Riedler, and K. D. Rendulic, Chem. Phys. Lett. **247**, 249 (1995).
[5] C. T. Rettner and D. J. Auerbach, Chem. Phys. Lett. **253**, 236 (1996).
[6] A. Groß, Surf. Sci. **363**, 1 (1996).

[7] M. Gostein and G. O. Sitz, J. Chem. Phys. **106**, 7378 (1997).

[8] A. Groß and M. Scheffler, Phys. Rev. B **57**, 2493 (1998).

[9] A. Groß, Appl. Phys. A **67**, 627 (1998).

[10] U. Muschiol, P. K. Schmidt, and K. Christmann, Surf. Sci. **395**, 182 (1998).

[11] P. K. Schmidt, K. Christmann, G. Kresse, J. Hafner, M. Lischka, and A. Groß, Phys. Rev. Lett. **87**, 096103 (2001).

[12] G.-J. Kroes, A. Groß, E. J. Baerends, M. Scheffler, and D. A. McCormack, Acc. Chem. Res. **35**, 193 (2002).

[13] A. Groß, ChemPhysChem **11**, 1374 (2010).

[14] A. Groß, S. Wilke, and M. Scheffler, Phys. Rev. Lett. **75**, 2718 (1995).

[15] A. Groß and M. Scheffler, Chem. Phys. Lett. **263**, 567 (1996).

[16] G.-J. Kroes, E. J. Baerends, and R. C. Mowrey, Phys. Rev. Lett. **78**, 3583 (1997).

[17] R. A. Olsen, G. J. Kroes, O. M. Løvvik, and E. J. Baerends, J. Chem. Phys. **107**, 10652 (1997).

[18] A. Groß, Surf. Sci. Rep. **32**, 291 (1998).

[19] G.-J. Kroes, Prog. Surf. Sci. **60**, 1 (1999).

[20] H. F. Busnengo, W. Dong, and A. Salin, Chem. Phys. Lett. **320**, 328 (2000).

[21] C. Crespos, H. F. Busnengo, W. Dong, and A. Salin, J. Chem. Phys. **114**, 10954 (2001).

[22] H. F. Busnengo, W. Dong, P. Sautet, and A. Salin, Phys. Rev. Lett. **87**, 127601 (2001).

[23] N. Pineau, H. F. Busnengo, J. C. Rayez, and A. Salin, J. Chem. Phys. **122**, 214705 (2005).

[24] A. Lozano, A. Groß, and H. F. Busnengo, Phys. Chem. Chem. Phys. **11**, 5814 (2009).

[25] H. F. Busnengo, E. Pijper, M. F. Somers, G. J. Kroes, A. Salin, R. A. Olsen, D. Lemoine, and W. Dong, Chem. Phys. Lett. **356**, 515 (2002).

[26] D. M. Bird, Faraday Discuss. **110**, 333 (1998).

[27] C. M. Wei, A. Groß, and M. Scheffler, Phys. Rev. B **57**, 15572 (1998).

[28] B. Hammer, Phys. Rev. B **63**, 205423 (2001).

[29] P. Broqvist, L. M. Molina, H. Grönbeck, and H. B., J. Catal. **227**, 217 (2004).

[30] M. Lischka and A. Groß, Phys. Rev. B **65**, 075420 (2002).

[31] M. Lischka, C. Mosch, and A. Groß, Surf. Sci. **570**, 227 (2004).

[32] A. Groß, C. M. Wei, and M. Scheffler, Surf. Sci. **416**, L1095 (1998).

[33] A. Groß and A. Dianat, Phys. Rev. Lett. **98**, 206107 (2007).

[34] A. Lozano, A. Groß, and H. F. Busnengo, Phys. Rev. B **81**, 121402(R) (2010).

[35] Y. Xiao and W. Dong, Phys. Rev. B **83**, 125418 (2011).

[36] F. Ahmed, M. K. Alam, R. Miura, A. Suzuki, H. Tsuboi, N. Hatakeyama, A. Endou, H. Takaba, M. Kubo, and A. Miyamoto, Catal. Today **164**, 16 (2011).

[37] T. Mitsui, M. K. Rose, E. Fomin, D. F. Ogletree, and M. Salmeron, Nature **422**, 705 (2003).

[38] T. Mitsui, M. K. Rose, E. Fomin, D. F. Ogletree, and M. Salmeron, Surf. Sci. **540**, 5 (2003).

[39] N. Lopez, Z. Lodziana, F. Illas, and M. Salmeron, Phys. Rev. Lett. **93**, 146103 (2004).

[40] R. J. Behm, K. Christmann, G. Ertl, and M. A. Van Hove, J. Chem. Phys. **73**, 2984 (1980).

[41] G. Kresse and J. Furthmüller, Phys. Rev. B **54**, 11169 (1996).

[42] J. P. Perdew, J. A. Chevary, S. H. Vosko, K. A. Jackson, M. R. Pederson, D. J. Singh, and C. Fiolhais, Phys. Rev. B **46**, 6671 (1992).

[43] D. Vanderbilt, Phys. Rev. B **41**, 7892 (1990).

[44] G. Kresse and J. Hafner, J. Phys.: Condens. Matter **6**, 8245 (1994).

[45] L. Verlet, Phys. Rev. **159**, 98 (1967).

[46] P. M. Agrawal, A. N. A. Samadh, L. M. Raff, M. T. Hagan, S. T. Bukkapatnam, and R. Komanduri, J. Chem. Phys. **123**, 224711 (2005).

[47] A. Groß and M. Scheffler, J. Vac. Sci. Technol. A **15**, 1624 (1997).

[48] S. Wilke, D. Hennig, R. Löber, M. Methfessel, and M. Scheffler, Surf. Sci. **307**, 76 (1994).

[49] S. Wilke and M. Scheffler, Phys. Rev. B **53**, 4926 (1996).

[50] S. H. Kim, H. L. Meyerheim, J. Barthel, J. Kirschner, J. Seo, and J.-S. Kim, Phys. Rev. B **71**, 205418 (2005).

[51] C. Resch, H. F. Berger, K. D. Rendulic, and E. Bertel, Surf. Sci. **316**, L1105 (1994).

[52] W. Dong and J. Hafner, Phys. Rev. B **56**, 15396 (1997).

[53] W. Dong, V. Ledentu, P. Sautet, A. Eichler, and J. Hafner, Surf. Sci. **411**, 123 (1998).

[54] S. Lorenz, A. Groß, and M. Scheffler, Chem. Phys. Lett. **395**, 210 (2004).

[55] S. Lorenz, M. Scheffler, and A. Groß, Phys. Rev. B **73**, 115431 (2006).

[56] A. Groß and M. Scheffler, Phys. Rev. B **61**, 8425 (2000).

[57] B. Berberich and A. Groß, Phys. Rev. B **82**, 195408 (2010).

[58] A. Roudgar and A. Groß, J. Electroanal. Chem. **548**, 121 (2003).

[59] V. Ledentu, W. Dong, P. Sautet, G. Kresse, and J. Hafner, Phys. Rev. B **57**, 12482 (1998).

[60] T. Engel and H. Kuipers, Surf. Sci. **90**, 162 (1979).

[61] M. Kiskinova and G. Bliznakov, Surf. Sci. **123**, 61 (1982).

[62] A. Groß, Phys. Rev. Lett. **103**, 246101 (2009).

[63] H. F. Busnengo, A. Salin, and W. Dong, J. Chem. Phys. **112**, 7641 (2000).

[64] A. Groß and M. Scheffler, Chem. Phys. Lett. **256**, 417 (1996).

[65] M. A. Di Cesare, H. F. Busnengo, W. Dong, and A. Salin, J. Chem. Phys. **118**, 11226 (2003).

[66] A. Dianat and A. Groß, J. Chem. Phys. **120**, 5339 (2004).

[67] A. Dianat, S. Sakong, and A. Groß, Eur. Phys. J. B **45**, 425 (2005).

[68] D. A. McCormack, R. A. Olsen, and E. J. Baerends, J. Chem. Phys. **122**, 194708 (2005).